Forecasted weakening of Atlantic Overturning Circulation could amplify future relative sea-level rise in the Mediterranean: a review of climate and tide-gauge data links

Nick Marriner[1*], David Kaniewski[2,3*], Majid Pourkerman[4], Matteo Vacchi[5], Daniele Melini[6], Martin Seeliger[7], Christophe Morhange[8,9] & Giorgio Spada[10]

1. CNRS, ThéMA, Université de Franche-Comté, UMR 6049, MSHE Ledoux, 32 rue Mégevand, 25030 Besançon Cedex, France

2. TRACES, UMR 5608 CNRS, Université Toulouse Jean Jaurès, Maison de la Recherche, 5 allées A. Machado 31058 Toulouse Cedex 9, France

3. Département de Biologie et Géosciences, Université Paul Sabatier - Toulouse 3, Toulouse cedex 9, France

4. Iranian National Institute for Oceanography and Atmospheric Science (INIOAS), Tehran, Iran

5. Dipartimento di Scienze della Terra, University of Pisa, Italy

6. Istituto Nazionale di Geofisica e Vulcanologia, 00143 Rome, Italy

7. Department of Physical Geography, Goethe-University Frankfurt, Frankfurt am Main, 60438, Germany

8. Aix Marseille Université, CNRS, IRD, INRA, Collège de France, CEREGE, 13545 Aix-en-Provence Cedex 04, France

9. EPHE-Section des Sciences Historiques et Philologiques, AOROC, UMR 8546 - Archéologie et Philologie d'Orient et d'Occident, CNRS/PSL, Ecole Normale Supérieure, 75230 Paris Cedex 5, France

10. Dipartimento di Fisica e Astronomia (DIFA), Settore Geofisica, Alma Mater Studiorum Università di Bologna, 40126 Bologna BO, Italy

* These authors contributed equally to this work

This is a pre-copyedited PDF of an article accepted for publication in Earth-Science Reviews following peer review. The version of record [Nick Marriner, David Kaniewski, Majid Pourkerman, Matteo Vacchi, Daniele Melini, Martin Seeliger, Christophe Morhange, Giorgio Spada, Forecasted weakening of Atlantic overturning circulation could amplify future relative sea-level rise in the Mediterranean: A review of climate and tide-gauge data links, Earth-Science Reviews, Volume 242, 2023, 104456] is available online at https://doi.org/10.1016/j.earscirev.2023.104456

Abstract

Sea-level rise is one of the most significant and perceptible consequences of global warming because it affects natural environments and coastal anthroposcapes at human timescales, particularly in sediment-starved littoral contexts. Within this framework, improvements in understanding the projection of sea-level rise require better knowledge of regional changes. Here we focus on the recent sea-level history of the Mediterranean Sea, an area characterized by a densely populated coast and where climate variability is larger, and the rate of sea-level rise higher than the global average. We produce a spatially-averaged Mediterranean relative sea-level (RSL) time series, based on 138 tide-gauge records, stretching back to the late 1800s, indicating that Mediterranean RSL has risen by ~24 cm in the past ~140 years. At interdecadal timescales and beyond, we find that Mediterranean relative sea-level rising rates (RSLRR) are significantly influenced by the strength of the Atlantic Multidecadal Oscillation (AMO) and the Atlantic Meridional Overturning Circulation (AMOC). Climate-model predictions of a weakened Atlantic overturning circulation in the coming decades, slowing and diminishing North Atlantic heat transport, has the potential to accentuate Mediterranean rising rates, with significant implications for the basin's coastal societies, infrastructure and economies. We conservatively estimate that a 0.1°C decrease in AMO sea surface temperatures can accentuate Mediterranean RSLRR by up to -0.61±0.5 mm yr^{-1}. Future coastal management and adaptation policies must assimilate these findings into local/regional-scale impact and vulnerability assessments.

Introduction

Reconstructing regional sea-level histories in semi-enclosed basins like the Mediterranean Sea is important for understanding the climate system and to prepare seaboard communities under threat from coastal erosion and increased flooding. In recent decades, the retreat of Mediterranean coastlines has been amplified by a drastic decrease in littoral sediment budgets and by rapid urbanization (Anthony et al., 2014), but there is a paucity of empirical data on Mediterranean coastal response to high rates of relative sea-level rise (RSLR), given the limited observation period of real-time geodetic measurements (Bonaduce et al., 2016). The densely populated Mediterranean region faces significant threats from RSLR and coastal erosion, given that human settlements, cultural heritage sites, agrosystems, anthroposcapes, and coastal infrastructure are all situated in limited coastal spaces (Neumann et al., 2015; Cramer et al., 2018; Reimann et al., 2018). The coastal population in this area has grown from approximately 100 million in 1980 to around 150 million in 2005, and it is projected to reach approximately 200 million by 2030 (Plan and Bleu, 2020). Artificial land cover is estimated to account for approximately 40% of the Mediterranean's coastal zone (Plan and Bleu, 2020).

The Mediterranean Sea is a semi-enclosed basin and its level is mediated by the local freshwater balance, exchanges with adjoining basins, steric changes and Glacial Isostatic Adjustment (Tsimplis and Rixen, 2002; Calafat et al., 2012; Galassi and Spada, 2014; Spada and Melini, 2021). Mediterranean RSLR is currently accelerating – levels have increased by >3.5 cm in the past 10 years (in relation to the 1980-1999 mean) – and projected median values could increase by 30 to 100 cm by 2100 (1994-2014 baseline), depending on the greenhouse gas emission scenario (I.P.C.C. et al.,

2021). Several studies have addressed the interannual variability of Mediterranean Sea level (Tsimplis et al., 2009; Tsimplis et al., 2011), but few investigations have sought to compile a basin-wide average and compare this to regional climate records. The period since the late 1800s is particularly pertinent in probing the RSL-climate link because it spans both the cool global temperatures of the late Little Ice Age (e.g. low solar irradiance) and the global warming of the 20th and 21st centuries (e.g. human-induced change, Neukom et al., 2014). One further factor, less understood, is the acceleration/deceleration in Mediterranean RSL due to dynamic responses to North Atlantic Ocean Circulation, for example, a potential slowdown in the Gulf Stream and Atlantic Meridional Overturning Circulation (Rahmstorf et al., 2015; Boers, 2021; Caesar et al., 2021) (AMOC), suggested to play a role in driving RSL changes along the eastern seaboard of North America (Bingham and Hughes, 2009; Ezer et al., 2013; Little et al., 2017). For instance, Piecuch et al. (2019) found a correlation between the AMOC at 26.5N and sea level along the New England coast, but this relationship is not causative and stems from synchronized but physically distant atmospheric influences connected to the North Atlantic Oscillation. In contrast, Volkov et al. (2019a) demonstrated that the AMOC's impact on the U.S. east coast sea level change is mediated through the ocean heat divergence/convergence on a gyre scale.

At present, satellite altimetry data only exist for the past four decades, making it extremely challenging to evaluate longer-term links between Mediterranean RSLR and climate change. To address this knowledge gap, we here use 138 tide-gauge records (Fig. 1) to produce a composite RSL curve for the Mediterranean Sea (Fig. S1). The quality and the continuity of Mediterranean tide-gauge measurements over time

renders the data reliable for long-term trend analysis. We compare and contrast it with decadal to interdecadal variability in climate dynamics.

Methods

The Mediterranean basin is monitored by a large number of tide gauges, some of which span >100 years. We compiled 138 Mediterranean records from the Permanent Service for Mean Sea Level (PSMSL, https://www.psmsl.org/), at an annual resolution (Figs. S1-S5). Fig. 1 displays the spatial distribution of the tide gauges used in the database, which range in temporal length from 3 to 135 (Marseille) years. Records with significant quality control issues were not included. All data were corrected for Glacial Isostatic Adjustment (GIA) using the recent ICE-7G model (Roy and Peltier, 2015; 2017) (Fig. 1), which has been recently validated by Roy and Peltier (2018) in a regional test for the Mediterranean basin. To obtain GIA model predictions, the ICE-7G model has been implemented in the Sea-Level Equation solver SELEN^4 (Spada and Melini, 2019). The Sea Level Equation has been solved on a global grid with spatial resolution of ~40 km, including harmonic terms up to the maximum degree Lmax = 512 which corresponds to a minimum wavelength of ~80 km on the Earth surface. To account for GIA modeling uncertainties, we also tested other GIA models, including the ICE-6G(VM5a) global model developed by Peltier et al. (2015) and one of the models developed by the Australian National University research group (Lambeck et al., 2003, Nakada and Lambeck, 1987), which has been specifically employed in the Mediterranean (Lambeck and Purcell, 2004). Model choice did not significantly alter the results due to the short nature of the time series and because the scatter between the different models is smaller than the uncertainties in the RSL trend (Fig. S6; see Spada and Melini, 2021 for a discussion). The individual GIA-corrected tide-gauge

records were subsequently summed and averaged to generate a basin-wide record of Mediterranean RSL and RSLRR. We also calculated a composite rising-rate time series using moving time windows of 20, 25 and 30 years. Potential sources of data bias exist, including for example: (i) the strong concentration of tide gauges on the northern and eastern coasts of the Mediterranean, with very few records from the Mediterranean coast of North Africa, and (ii) vertical land motion of tectonic or anthropogenic origin that may affect tide-gauge records at specific sites (Buble et al., 2010; Faccenna, 2014).

To explore the role of steric-driven changes in driving RSL at tide-gauge stations, annual Sea Surface Temperatures (SST) were extracted from the International Comprehensive Ocean-Atmosphere Data Set (ICOADS) (https://icoads.noaa.gov). The SST data were used to establish a spatially averaged record of Mediterranean SST. We also compared and contrasted the Mediterranean RSLR data with various high-resolution palaeoclimate datasets including: (i) Mediterranean air surface temperatures (Osborn and Jones, 2014); (ii) the Atlantic Multidecadal Oscillation (Enfield et al., 2001) (https://psl.noaa.gov/data/timeseries/AMO/); and (iii) Atlantic Meridional Overturning Circulation (Caesar et al., 2018).

To assess the quality of the RSL and SST time series, we randomly sampled 40, 60, 80, 100, and 120 records from the total of 138 used to construct the two time series. The overall variability between the sub-sampled time series and the "all sites" series for the RSL record was <5%, with a mean of 1.57±1.1% (Fig. S7A). For the SST record, the overall variability was <4%, with a mean of 1.25±0.6% (Fig. S7B). Based on these

results, we are confident that both time series effectively capture the RSL and SST histories of the Mediterranean basin.

Statistical analyses were performed using Xl-Stat2019 (https://www.xlstat.com), R 4.1.0 (Team, 2017) and PAST 4.08 (Hammer et al., 2001). To explore the links between RSL, SST and air surface temperature, cross correlations ($P < 0.05$) were calculated, shown in Fig. 2. Cross-correlation is a statistical technique used to measure the similarity between two time series as a function of the time shift (i.e. lag) between them (Kaniewski et al., 2008). It is commonly used in time series analysis where the timing relationship between two signals is important (e.g. Fiorillo and Doglioni, 2010). The technique involves computing the correlation coefficient (CC) between the two time series as they are shifted in time relative to each other. The correlation coefficient is a measure of the degree of linear relationship between the two time series. A value of 1 indicates a perfect positive correlation (i.e., as one time series increases, so does the other), a value of -1 indicates a perfect negative correlation (i.e., as one time series increases, the other decreases), and a value of 0 indicates no correlation. The cross-correlation function can help determine the lag between two time series, which can be used to identify causal relationships or synchronization between the signals. The maximum value of the cross-correlation function indicates the optimal lag, where the two signals are most highly correlated. We consider positive and negative correlation coefficients with a focus on the Lag0 value, using 0.5 or -0.5 as the significant threshold. Non-significant values indicate no correlation.

Sinusoidal regressions were used to model periodicities in the time series (the Pvalue, based on an F-test, gives the significance of the fit). The regressions (RSL rising rate,

Atlantic Multidecadal Oscillation and Atlantic Meridional Overturning Circulation) were then compared and contrasted. The link between RSL rising rate and Atlantic Multidecadal Oscillation was tested, ranking the Atlantic Multidecadal Oscillation scores in ascending order and retaining the associated RSL rising rate values. Averages were calculated and are plotted with their confidence intervals. Linear and polynomial models (Pvalue < 0.001) were added. Variations in RSL rising rate were then calculated for a steady increase of 0.1°C in the Atlantic Multidecadal Oscillation. The same process was applied in testing the relationship between the RSL rising rate and the Atlantic Meridional Overturning Circulation. Variations in RSL rising rate were then calculated for a steady increase of 0.5°C in the Atlantic Meridional Overturning Circulation (Fig. 3).

Results and discussion

Anatomy of Mediterranean RSL changes since the late 1880s

Mediterranean RSL has risen by >20 cm since the late 1800s (1884 to 2010 = 243 mm rise), largely consistent with the global average (Dangendorf et al., 2019). Since 1884, RSL in 93 % of years has been inferior to the 2010-2019 mean. Fig. 2 plots (A) a basin-wide average of Mediterranean RSL based on tide-gauge records between 1884-2019; (B) a spatial average of Mediterranean Sea Surface Temperatures (SSTs) from the tide gauge sites; and (C) Mediterranean air-surface temperatures (T°C). Strong rising trends are observed in all three data series. Mediterranean RSL shows an average rising trend of 1.78 ± 0.27 mm yr^{-1} for the period 1884–2019, from minima during the late 1800s (6896 ± 46 mm in the period 1884-1889) to maxima during the 2010s (7044 ± 74 mm in the period 2010-2019). Over the same period, Mediterranean SSTs have

risen at an average rate of 0.03 ± 0.007 °C yr^{-1} and Mediterranean air surface temperature at 0.02 ± 0.002 °C yr^{-1}.

To explore the trend components, we applied a smoother (10-year moving average) to all three datasets before looking for statistically significant breaks in the data using change-point methods (Fig. 3). Change-point detection is a particularly effective tool in probing shifts or shocks in environmental time series (Cahill et al., 2015). The method divides time series into segments, where the values within each section have a similar mean and standard deviation. The results reveal two significant change points in the RSL data (1898, 1956), three for the Mediterranean SST data (1896, 1950, 2001) and two for the Mediterranean air surface temperature data (1926, 2001). Although the early 2000s change point is not detected in the Mediterranean RSL data, there is close phasing of this time series with the Mediterranean SST data in particular. Three broad plateaus are delineated in the RSL trends. Period 1 runs from the late 1880s until 1897, with average RSL of -152 ± 45 mm and an SST of 16.75 ± 0.51°C. This period corresponds to lower RSL and gradual SST warming at the end of the Little Ice Age (Mann et al., 2009; Morice et al., 2021; Marriner et al., 2022). The warming of SSTs at the end of the Little Ice Age led to the melting of glaciers and ice sheets, the thermal expansion of seawater (Kemp et al., 2011) and changes in Atlantic Ocean circulation patterns and water distribution patterns which contributed to the observed sea-level rise in the Mediterranean (e.g. Vacchi et al., 2022). Period 2 spans 1898 to 1955, with average RSL of -85 ± 51 mm and a SST of 17.51 ± 0.84°C (Fig. 3). Period 3 encompasses 1956 to 2019, with average RSL of -27 ± 66 mm and an SST of 18.75 ± 1.16°C. We note a significant jump in Mediterranean RSL of >100 mm between 1950

and 1960 which appears to translate a lagged response to significant Mediterranean SST warming during the mid-1940s, consistent with the Great Acceleration (Steffen et al., 2015). The Great Acceleration refers to the significant increase in human activities and their impacts on the Earth's systems since the mid-20th century (Steffen et al., 2015). It includes various aspects such as population growth, urbanization, industrialization, and agricultural intensification, which have engendered a range of environmental changes and challenges, including climate change, biodiversity loss, and pollution. Within this context, RSL rise in the Mediterranean has been affected by the increase in global temperatures, which has led to the melting of land-based ice sheets and glaciers and the steric expansion of seawater (Bonaduce et al., 2016). One further contributing factor could be a weakening in Atlantic Ocean overturning circulation, beginning in the 1950s, through mass exchanges with the North Atlantic (Volkov et al., 2019b). While Volkov et al. (2019b) put forth a potential explanation for how shifts in the AMOC could impact sea level in the Mediterranean, they did not examine the potential effects of a decline in the AMOC since the mid-20th century.

North Atlantic thermohaline pacing of Mediterranean RSL rising rates

To probe oscillations in the Mediterranean RSL record, a composite rising-rate time series was calculated. This was done in order to minimize the purely random variability that dominates the time series at high frequencies, while retaining most of the variability at decadal and longer periods. Previous studies have demonstrated that nonseasonal fluctuations in Mediterranean RSL can be attributed to wind-driven mass changes and exchanges with the Atlantic Ocean (Landerer and Volkov, 2013; Tsimplis et al., 2013). To focus on the interdecadal variability in rising rates, this time series was further smoothed using 10 to 25-year moving averages. Average Mediterranean

RSLRRs for the whole sequence (1884 to 2019) are 1.24 ± 0.48 mm/yr, with a minimum of -1.05 ± 0.15 mm yr^{-1} in 1946 and a maximum of 3.12 ± 0.17 mm yr^{-1} in 1974. The data presented in Fig. 4 manifest a clear ~60-year cycle, characterized by: (i) two phases of RSL decrease spanning the early 1920s to the late 1940s (with the peak change of -1.05 ± 0.15 mm yr^{-1} occurring in 1946) and the late 1970s to the late 1990s (peak change of -0.02 ± 0.81 mm yr^{-1} in 1997); and (ii) two periods of contrasting RSL acceleration encompassing the early 1950s to the early 1970s (maximum acceleration of 3.12 ± 0.17 mm yr^{-1} in 1974) and the early 2000s to present (maximum acceleration of 1.53 ± 0.1 mm yr^{-1} in 2018). Multiple linear regression analyses show that the Mediterranean's multidecadal RSLRR record manifests highly significant anti-phasing (inverse fit r = -0.8; permutation p = 0.0001) with records of the Atlantic Meridional Oscillation, whereby a warmer (cooler) AMO is associated with lower (higher) RSLRR in the Mediterranean. For AMOC, the Mediterranean data also show significant anti-phasing (r = -0.5; permutation p = 0.0001). Since the early 1990s, satellite altimetry data show that AMO/AMOC affect basin-mean surface height in the Mediterranean Sea via the Gibraltar inflow transport (von Schuckmann et al. 2016; Meli et al., 2023). The AMO refers to a long-term pattern of variability in the temperature of the Atlantic Ocean (Marullo et al., 2011), while the AMOC refers to the movement of ocean currents that bring warm surface water from the tropics to the North Atlantic, where it cools and sinks to form deep currents that eventually circulate back to the tropics. One way that the AMO and AMOC can affect the climate and oceanography of the Mediterranean Sea is by influencing the amount of water that flows into the basin through the Strait of Gibraltar (Iona et al., 2018). The flow of water through the Strait of Gibraltar is an important part of the AMOC, as it helps to regulate the exchange of heat and salt between the Atlantic and Mediterranean. For example,

recent remote sensing data found that during periods of high AMO and strong AMOC, the inflow transport into the Mediterranean tended to be weaker, leading to lower sea levels in the basin (e.g. von Schuckmann et al. 2016). Conversely, during periods of low AMO and weak AMOC, the inflow transport of warm and saltier water tended to be stronger, leading to higher Mediterranean sea levels. Variations in the amount, temperature and salinity of water that flows through the Strait of Gibraltar therefore have significant impacts on the mean sea level of the Mediterranean Sea, which can in turn affect coastal communities and ecosystems (Lionello et al., 2006). Nonetheless, our understanding of these mechanisms at longer interdecadal timescales was, until now, unclear.

Recent investigations suggest that the AMO is significantly linked to the AMOC which plays a major role in connecting external forcing with North Atlantic SSTs. At interdecadal timescales (10-30 years), a model-based study by Kim and colleagues (Kim et al., 2021) demonstrated that AMO and the AMOC establish a self-sustaining oscillatory mode, whereby the AMOC induces a positive AMO through meridional heat transport, but with a time lag of ~7 years as the AMOC anomalies spatially propagate southwards in the Atlantic basin. After then, the AMO reduces the density in the main sinking region and induces the negative phase of the AMOC, which results in the second half of the cycle. At multi-decadal timescales (>50 years), the AMO and the AMOC are almost in phase because the AMOC is spatially stationary, leading to a pan-Atlantic surface warming.

Caesar et al., (2018) have elucidated a generally weaker AMOC between 1965–1995, resulting in weaker northward heat transport and decreasing North Atlantic SSTs at

high northern latitudes (and decreasing Mediterranean RSLRR). This contrasts with a stronger AMOC around 1930–1965 and after 1995 (Caesar et al., 2018), underpinning warmer North Atlantic SSTs and increasing Mediterranean RSLRR. An increase (decrease) of sea-level pressure in the center of the North Atlantic subtropical gyre is associated with a strengthening (weakening) of westerly winds in the midlatitudes and trade winds in the subtropics. The trade winds drive northward (southward) Ekman transport anomalies that directly strengthen (weaken) the AMOC (Frajka-Williams et al., 2016; Wang et al., 2019). These modifications are linked with southwestward (northeastward) wind anomalies along the northwest African coast and westward (eastward) wind anomalies over the Strait of Gibraltar, which, coupled with a weaker (stronger) Azores Current, pump water out of (into) the Mediterranean Sea, therefore lowering (raising) its sea level (Fig. 5; Volkov and Landerer, 2015; Volkov et al., 2019a,b). Short time series have demonstrated that these winds are able to modify the sea-level gradient along the strait, leading to barotropic sea-level fluctuations in the Mediterranean (Volkov et al., 2019b). The redistribution mechanism of North Atlantic heat, conveying energy from lower to mid and higher latitudes, highlights the importance of the thermosteric and thermohaline components in mediating both North Atlantic and Mediterranean sea-level variability. A recent study investigating late Holocene RSL variations in the Western Mediterranean highlighted a previously unrecognized variability in the basin's sea-level change rates that were correlated with the occurrence of major regional-scale cooling/warming episodes (Vacchi et al., 2021). We hypothesize that past changes in the strength of the Atlantic Ocean Overturning Circulation could have been key in modulating this centennial to millennial-scale variability.

Conclusion

The findings of this study suggest that better exploration of regional climatic parameters, mediating variability in Mediterranean RSL rising rates, is required to produce robust predictions of Mediterranean RSLR in the coming century. Regional forecasts for the Mediterranean could deviate markedly from global-scale scenarios, particularly within the context of a projected slowdown in AMOC in future decades, already at its weakest point in the last 1000 years (Caesar et al., 2021). This has significant implications for the near-future resilience of both natural and human-modified Mediterranean coasts, characterized by rapid demographic, social, economic and environmental change (Furlan et al., 2021). Current and future coastal management and adaptation policies, such as those included in the Integrated Coastal Zone Management (ICZM) Protocol of the Barcelona Convention (MedECC, 2020), must integrate these findings into local/regional-scale impact and vulnerability assessments for sustainable coastal planning in the 21st century (Satta et al., 2017). These data provide a regional baseline for present and future Mediterranean RSLR processes and prediction studies.

Acknowledgements

Financial support was provided by the MITI-CNRS "*Evénements rares*" project AQUASANMARCO.

References

Anthony, E., Marriner, N., Morhange, C., 2014. Human influence and the changing geomorphology of Mediterranean deltas and coasts over the last 6000 years: From progradation to destruction phase? Earth-Sci. Rev. 139, 336–361.

Bingham, R., Hughes, C.W., 2009. Signature of the Atlantic meridional overturning circulation in sea level along the east coast of North America. Geophys. Res. Lett. 36, 02603.

Boers, N., 2021. Observation-based early-warning signals for a collapse of the Atlantic Meridional Overturning Circulation. Nat. Clim. Change 11, 680–688.

Bonaduce, A., Pinardi, N., Oddo, P., Spada, G., Larnicol, G., 2016. Sea-level variability in the Mediterranean Sea from altimetry and tide gauges. Clim Dyn 47, 2851–2866.

Buble, G., Bennett, R.A., Hreinsdóttir, S., 2010. Tide gauge and GPS measurements of crustal motion and sea level rise along the eastern margin of Adria. J Geophys Res 115, 02404.

Caesar, L., McCarthy, G.D., Thornalley, D.J.R., Cahill, N., Rahmstorf, S., 2021. Current Atlantic Meridional Overturning Circulation weakest in last millennium. Nat. Geosci. 14, 118–120.

Caesar, L., Rahmstorf, S., Robinson, A., Feulner, G., Saba, V., 2018. Observed fingerprint of a weakening Atlantic Ocean overturning circulation. Nature 556, 191–196.

Cahill, N., Rahmstorf, S., Parnell, A.C., 2015. Change points of global temperature. Environ. Res. Lett. 10, 084002.

Calafat, F.M., Chambers, D.P., Tsimplis, M.N., 2012. Mechanisms of decadal sea level variability in the eastern North Atlantic and the Mediterranean Sea. J. Geophys. Res. 117, 09022.

Cramer, W., Guiot, J., Fader, M., Garrabou, J., Gattuso, J.-P., Iglesias, A., Lange, M.A., Lionello, P., Llasat, M.C., Paz, S., Peñuelas, J., Snoussi, M., Toreti, A., Tsimplis, M.N., Xoplaki, E., 2018. Climate change and interconnected risks to sustainable development in the Mediterranean. Nat. Clim. Change 8, 972–980.

Dangendorf, S., Hay, C., Calafat, F.M., Marcos, M., Piecuch, C.G., Berk, K., Jensen, J., 2019. Persistent acceleration in global sea-level rise since the 1960s. Nat. Clim. Change 9, 705–710.

Enfield, D.B., Mestas-Nunez, A.M.T., J, P., 2001. The Atlantic Multidecadal Oscillation and its relationship to rainfall and river flows in the continental U.S. Geophys. Res. Lett. 28, 2077–2080.

Ezer, T., Atkinson, L.P., Corlett, W.B., Blanco, J.L., 2013. Gulf Stream's induced sea level rise and variability along the U.S. -Atl. Coast J Geophys Res Oceans 118, 685–697.

Faccenna, C., 2014. Mantle dynamics in the Mediterranean. Rev Geophys 52, 283–332.

Fiorillo, F., Doglioni, A., 2010. The relation between karst spring discharge and rainfall by cross-correlation analysis (Campania, southern Italy). Hydrogeol J 18, 1881–1895.

Frajka-Williams, E., Meinen, C.S., Johns, W.E., Smeed, D.A., Duchez, A., Lawrence, A.J., Cuthbertson, D.A., McCarthy, G.D., Bryden, H.L., Baringer, M.O., Moat, B.I., Rayner, D., 2016. Compensation between meridional flow components of the Atlantic MOC at 26°N. Ocean Sci. 12, 481–493.

Furlan, E., Dalla Pozza, P., Michetti, M., Torresan, S., Critto, A., Marcomini, A., 2021. Development of a Multi-Dimensional Coastal Vulnerability Index: Assessing vulnerability to inundation scenarios in the Italian coast. Sci. Total Environ. 772, 144650.

Galassi, G., Spada, G., 2014. Sea-level rise in the Mediterranean Sea by 2050: Roles of terrestrial ice melt, steric effects and glacial isostatic adjustment. Glob. Planet. Change 123, 55–66.

Hammer, O., Harper, D.A.T., Ryan, P.D., 2001. PAST: Paleontological Statistics Software Package for Education and Data Analysis 4, 9.

Iona, A., Theodorou, A., Sofianos, S., Watelet, S., Troupin, C., Beckers, J.M., 2018. Mediterranean Sea climatic indices: Monitoring long-term variability and climate changes. Earth Syst. Sci. Data 10, 1829–1842.

I.P.C.C., V., P.Z., Pirani, A., Connors, S.L., Péan, C., Berger, S., Caud, N., Chen, Y., Goldfarb, L., Gomis, M.I., Huang, M., Leitzell, K., Lonnoy, E., 2021. Climate Change 2021: The Physical Science Basis. Contribution of Working Group I to the Sixth Assessment Report of the Intergovernmental Panel on Climate Change [Masson-Delmotte. Cambridge University Press, Cambridge, United Kingdom and New York, NY, USA.

Kaniewski, D., Paulissen, E., Van Campo, E., Al-Maqdissi, M., Bretschneider, J., Van Lerberghe, K., 2008. Middle East coastal ecosystem response to middle-to-late Holocene abrupt climate changes. Proc. Natl. Am. Soc.105, 13941–13946.

Kemp, A.C., Horton, B.P., Donnelly, J.P., Mann, M.E., Vermeer, M., Rahmstorf, S., 2011. Climate related sea-level variations over the past two millennia. Proc. Natl. Am. Soc. 108, 11017–11022.

Kim, H.-J., An, S.-I., Kim, D., 2021. Timescale-dependent AMOC–AMO relationship in an earth system model of intermediate complexity. Int. J. Climatol. 41, 3298–3306.

Lambeck, K., Purcell, A., Johnston, P., Nakada, M., Yokoyama, Y., 2003. Water-load definition in the glacio-hydro-isostatic sea level equation. Quat. Sci. Rev. 22, 309–318.

Lambeck, K., Purcell, A., 2004. Sea-level change in the Mediterranean Sea since the LGM: model predictions for tectonically stable areas. Quat. Sci. Rev. 24, 1969–1988.

Landerer, F.W., Volkov, D.L., 2013. The anatomy of recent large sea level fluctuations in the Mediterranean Sea. Geophys. Res. Lett. 40, 553–557.

Little, C.M., Piecuch, C.G., Ponte, R.M., 2017. On the relationship between the meridional overturning circulation, alongshore wind stress, and United States East Coast sea level in the Community Earth System Model Large Ensemble. J Geophys Res Oceans 122, 4554–4568.

Lionello, P., Malanotte-Rizzoli, P., Boscolo, R., 2006. Mediterranean climate variability. Elsevier.

Mann, M.E., Zhang, Z., Rutherford, S., Bradley, R.S., Hughes, M.K., Shindell, D., Ammann, C., Faluvegi, G., Ni, F., 2009. Global Signatures and Dynamical Origins of the Little Ice Age and Medieval Climate Anomaly. Science 326, 1256–1260.

Marullo, S., Artale, V., Santoleri, R., 2011. The SST multidecadal variability in the Atlantic-Mediterranean region and its relation to AMO. J. Climate 24, 4385–4401.

Marriner, N., Kaniewski, D., Pourkerman, M., Devillers, B., 2022. Anthropocene tipping point reverses long-term Holocene cooling of the Mediterranean Sea: A meta-analysis of the basin's Sea Surface Temperature records. Earth-Sci. Rev. 227, 103986.

MedECC, 2020. Climate and Environmental Change in the Mediterranean Basin – Current Situation and Risks for the Future. First Mediterranean Assessment Report, in: Cramer, W., Guiot, J., Marini, K. (Eds.), Union for the Mediterranean. Plan Bleu, UNEP/MAP, Marseille, France.

Meli, M., Camargo, C.M.L., Olivieri, M., Slangen, A.B.A., Romagnoli, C., 2023. Sea-level trend variability in the Mediterranean during the 1993–2019 period. Front. Mar. Sci. 10, 1150488.

Morice, C.P., Kennedy, J.J., Rayner, N.A., Winn, J.P., Hogan, E., Killick, R.E., Dunn, R.J.H., Osborn, T.J., Jones, P.D., Simpson, I.R., 2021. An Updated Assessment of Near-Surface Temperature Change From 1850: The HadCRUT5 Data Set. J. Geophys. Res. Atmospheres 126, 2019 032361.

Nakada, M., Lambeck, K., 1987. Glacial rebound and relative sea level variations: a new appraisal. Geophys. J. Int. 90, 171–224.

Neukom, R., Gergis, J., Karoly, D.J., Wanner, H., Curran, M., Elbert, J., González Rouco, F., Linsley, B.K., Moy, A.D., Mundo, I., Raible, C.C., Steig, E.J., Ommen, T., Vance, T., Villalba, R., Zinke, J., Frank, D., 2014. Inter-Hemispheric Temperature Variability over the Past Millennium. Nat. Clim. Change 4, 362–67.

Neumann, B., Vafeidis, A.T., Zimmermann, J., Nicholls, R.J., 2015. Future coastal population growth and exposure to sea-level rise and coastal flooding—A global assessment. PLoS ONE 10, 0118571.

Osborn, T.J., Jones, P.D., 2014. The CRUTEM4 land-surface air temperature data set: construction, previous versions and dissemination via Google Earth. Earth Syst. Sci. Data 6, 61–68.

Piecuch, C.G., Dangendorf, S., Gawarkiewicz, G.G., Little, C.M., Ponte, R.M., Yang, J., 2019. How is New England coastal sea level related to the Atlantic meridional overturning circulation at 26°N? Geophys. Res. Lett. 46, 5351–5360.

Peltier, W.R., Argus, D.F., Drummond, R., 2015. Space geodesy constrains ice age terminal deglaciation: The global ICE-6G C (VM5a) model. J. Geophys. Res. Solid Earth 120450–487.

Plan, U.N.E.P.A., Bleu, P., 2020. State of the Environment and Development in the Mediterranean.

Rahmstorf, S., Box, J.E., Feulner, G., Mann, M.E., Robinson, A., Rutherford, S., Schaffernicht, E.J., 2015. Exceptional twentieth-century slowdown in Atlantic Ocean overturning circulation. Nat. Clim. Change 5, 475–480.

Reimann, L., Vafeidis, A.T., Brown, S., Hinkel, J., Tol, R.S.J., 2018. Mediterranean UNESCO World Heritage at risk from coastal flooding and erosion due to sea-level rise. Nat. Commun. 9, 4161.

Roy, K., Peltier, W. R., 2015. Glacial isostatic adjustment, relative sea level history and mantle viscosity: reconciling relative sea level model predictions for the US East coast with geological constraints. Geophys. J. Int. 201(2), 1156-1181.

Roy, K., Peltier, W. R., 2017. Space-geodetic and water level gauge constraints on continental uplift and tilting over North America: regional convergence of the ICE-6G_C (VM5a/VM6) models. Geophys. J.l Int. 210(2), 1115-1142.

Roy, K., Peltier, W.R., 2018. Relative sea level in the Western Mediterranean basin: A regional test of the ICE-7G_NA (VM7) model and a constraint on Late Holocene Antarctic deglaciation. Quat. Sci. Rev. 183, 76–87.

Satta, A., Puddu, M., Venturini, S., Giupponi, C., 2017. Assessment of coastal risks to climate change related impacts at the regional scale: The case of the Mediterranean region. Int. J. Disaster Risk Reduct. 24, 284–296.

Spada, G., Melini, D., 2021. New estimates of ongoing sea level change and land movements caused by Glacial Isostatic Adjustment in the Mediterranean region. Geophys J Int 229, 2, 984–998.

Spada, G., Melini, D., 2019. SELEN4 (SELEN version 4.0): A Fortran program for solving the gravitationally and topographically self-consistent sea-level equation in glacial isostatic adjustment modeling. Geosci. Model Dev. 12, 5055–5075.

Steffen, W., Broadgate, W., Deutsch, L., Gaffney, O., Ludwig, C., 2015. The trajectory of the Anthropocene: The Great Acceleration. Anthr. Rev. 2, 81–98.

Team, R.C., 2017. R: A language and environment for statistical computing.

Tsimplis, M., Marcos, M., Colin, J., Somot, S., Pascual, A., Shaw, A., 2009. Sea level variability in the Mediterranean Sea during the 1990s on the basis of two 2d and one 3d model. J Mar Syst 78, 109–123.

Tsimplis, M., Spada, G., Marcos, M., Flemming, N., 2011. Multi-decadal sea level trends and land movements in the Mediterranean Sea with estimates of factors perturbing tide gauge data and cumulative uncertainties. Glob. Planet. Change 76, 63–76.

Tsimplis, M.N., Calafat, F.M., Marcos, M., Jordà, G., Gomis, D., Fenoglio-Marc, L., Struglia, M.V., Josey, S.A., Chambers, D.P., 2013. The effect of the NAO on sea level and on mass changes in the Mediterranean Sea: NAO effects on

Mediterranean Sea level. J Geophys Res Oceans 118, 944–952. https://doi.org/10.1002/jgrc.20078

Tsimplis, M.N., Rixen, M., 2002. Sea level in the Mediterranean Sea: The contribution of temperature and salinity changes. Geophys. Res. Lett. 29, 2136,. https://doi.org/10.1029/2002GL015870.

Vacchi, M., Joyse, K.M., Kopp, R.E., Marriner, N., Kaniewski, D., Rovere, A., 2021. Climate pacing of millennial sea-level change variability in the central and western Mediterranean. Nat. Commun. 12, 4013.

Volkov D.L., Landerer, F.W., 2015. Internal and external forcing of sea level variability in the Black Sea. Clim. Dyn. 45, 2633–2646.

Volkov, D.L., Lee, S.-K., Domingues, R., Zhang, H., Goes, M., 2019a. Interannual sea level variability along the southeastern seaboard of the United States in relation to the gyre-scale heat divergence in the North Atlantic. Geophys. Res. Lett. 46, 7481–7490.

Volkov, D.L., Baringer, M., Smeed, D., Johns, W., Landerer, F.W., 2019b. Teleconnection between the Atlantic Meridional Overturning Circulation and sea level in the Mediterranean Sea. J. Clim. 32, 935–955.

Volkov D.L., & F.W. Landerer (2015). Internal and external forcing of sea level variability in the Black Sea, Clim. Dyn. , doi:10.1007/s00382-015-2498-0.

von Schuckmann, K., Le Traon, P.-Y., Alvarez-Fanjul, E., Axell, L., Balmaseda, M., Breivik, L.-A., Brewin, R.J.W., Bricaud, C., Drevillon, M., Drillet, Y., Dubois, C., Embury, O., Etienne, H., Sotillo, M.G., Garric, G., Gasparin, F., Gutknecht, E., Guinehut, S., Hernandez, F., Juza, M., Karlson, B., Korres, G., Legeais, J.-F., Levier, B., Lien, V.S., Morrow, R., Notarstefano, G., Parent, L., Pascual, Á., Pérez-Gómez, B., Perruche, C., Pinardi, N., Pisano, A., Poulain, P.-M., Pujol, I.M., Raj, R.P., Raudsepp, U., Roquet, H., Samuelsen, A., Sathyendranath, S., She, J., Simoncelli, S., Solidoro, C., Tinker, J., Tintoré, J., Viktorsson, L., Ablain, M., Almroth-Rosell, E., Bonaduce, A., Clementi, E., Cossarini, G., Dagneaux, Q., Desportes, C., Dye, S., Fratianni, C., Good, S., Greiner, E., Gourrion, J., Hamon, M., Holt, J., Hyder, P., Kennedy, J., Manzano-Muñoz, F., Melet, A., Meyssignac, B., Mulet, S., Buongiorno Nardelli, B., O'Dea, E., Olason, E., Paulmier, A., Pérez-González, I., Reid, R., Racault, M.-F., Raitsos, D.E., Ramos, A., Sykes, P., Szekely, T., Verbrugge, N., 2016. The Copernicus Marine Environment Monitoring Service Ocean State Report. Journal of Operational Oceanography 9, s235–s320.

Wang, Z., Brickman, D., Greenan, B.J.W., 2019. Characteristic evolution of the Atlantic Meridional Overturning Circulation from 1990 to 2015: An eddy-resolving ocean model study. Deep Sea Res. Part Oceanogr. Res. Pap. 149, 103056.

Figure captions

Figure 1: Present-day rates of sea-level change in the Mediterranean area according to the ICE-7G Glacial Isostatic Adjustment (Roy and Peltier, 2015; 2017). The white dots denote the location of tide gauges used in this study.

Figure 2: (A) Composite Mediterranean RSL stack for the period 1880-2020, produced using the 138 tide-gauge stations used in this study. **(B)** Composite stack of SSTs at the studied tide-gauge stations. **(C)** Mediterranean air surface temperatures (Osborn and Jones, 2014). The three bottom insets show the cross-correlations between the three considered variables.

Figure 3: Change-point analysis of the Mediterranean RSL stack **(A)**, Mediterranean SSTs **(B)** and Mediterranean air surface temperatures **(C)**. **(D)** Juxtaposition of the different change points for the three time series.

Figure 4: (A & B) Mediterranean relative sea-level rising rates (RSLRR) compared with Atlantic Multi-decadal Oscillation Sea Surface Temperature (data from Enfield et al., 2001). **(C & D)** Mediterranean RSLRR versus Atlantic meridional overturning circulation Sea Surface Temperature (°C; data from Caesar et al., 2018).

Figure 5: Schematic explanation of the climate/thermocline mechanisms leading to RSL changes in the Mediterranean during phases of stronger **(A)** and weaker **(B)** AMOC.

Supplementary Data

Figure S1: Location of tide gauge stations used in the present study. The stations have been numbered 1 to 138 and sorted by longitude, with 1 being furthest west and 138 the station furthest east.

Figure S2: Temporal coverage of tide gauge records for stations 1 to 50.

Figure S3: Temporal coverage of tide gauge records for stations 51 to 100.

Figure S4: Temporal coverage of tide gauge records for stations 101 to 138.

Figure S5: Plot of Mediterranean RSL data from the 138 Mediterranean tide-gauge stations used in this study.

Figure S6: Present-day rates of sea level change in the Mediterranean area according to a set of Glacial Isostatic Adjustment models: **(A)** the ICE-6G model since the last glacial maximum (Peltier et al., 2015), **(B)** the ICE-6G model over the full last glacial cycle, **(C)** the ICE-7G model (Roy and Peltier, 2018) and **(D)** one of the models progressivley developed by the Australian National University (ANU) research group (Lambeck et al., 2003; Nakada and Lambeck, 1987). The white dots denote the location of tide gauges used in the study.

Fig. S7: Effects of random sampling on the reconstructed Relative Sea Level (RSL) (**A**) and Sea Surface Temperature (SST) (**B**) time series. The figure shows five sub-sampled time series of 40, 60, 80, 100, and 120 records, out of a total of 138 records. Our analysis indicates that the overall variability between the sub-sampled time series

and the "all sites" series was minimal. Specifically, for the RSL record, the overall variability was less than 5% (mean = 1.57 ± 1.1%), while for the SST record, the overall variability was less than 4% (mean = 1.25 ± 0.6%).

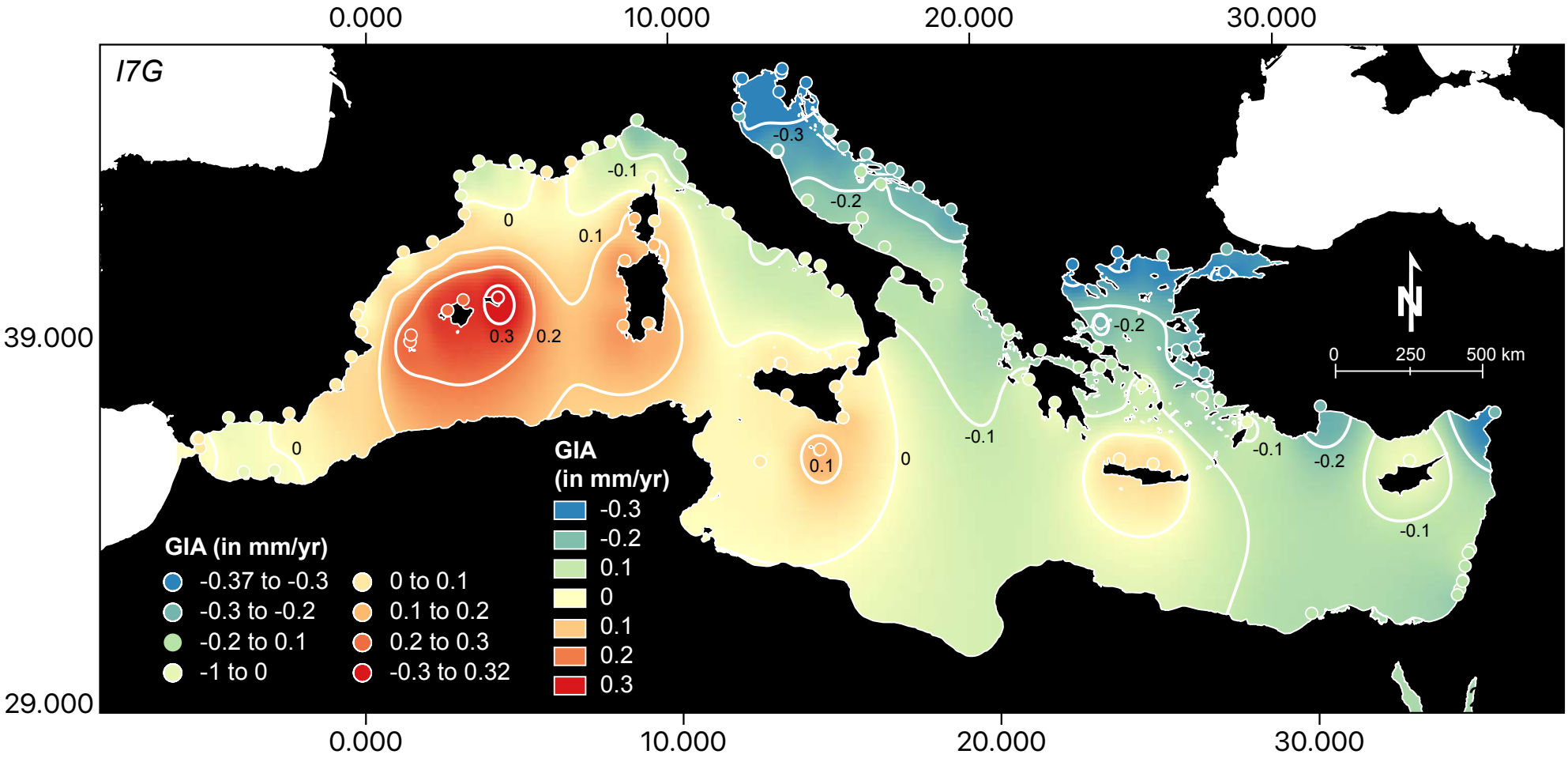

Figure 1: Present-day rates of sea-level change in the Mediterranean area according to the ICE-7G Glacial Isostatic Adjustment (Roy and Peltier, 2015; 2017). The white dots denote the location of tide gauges used in this study.

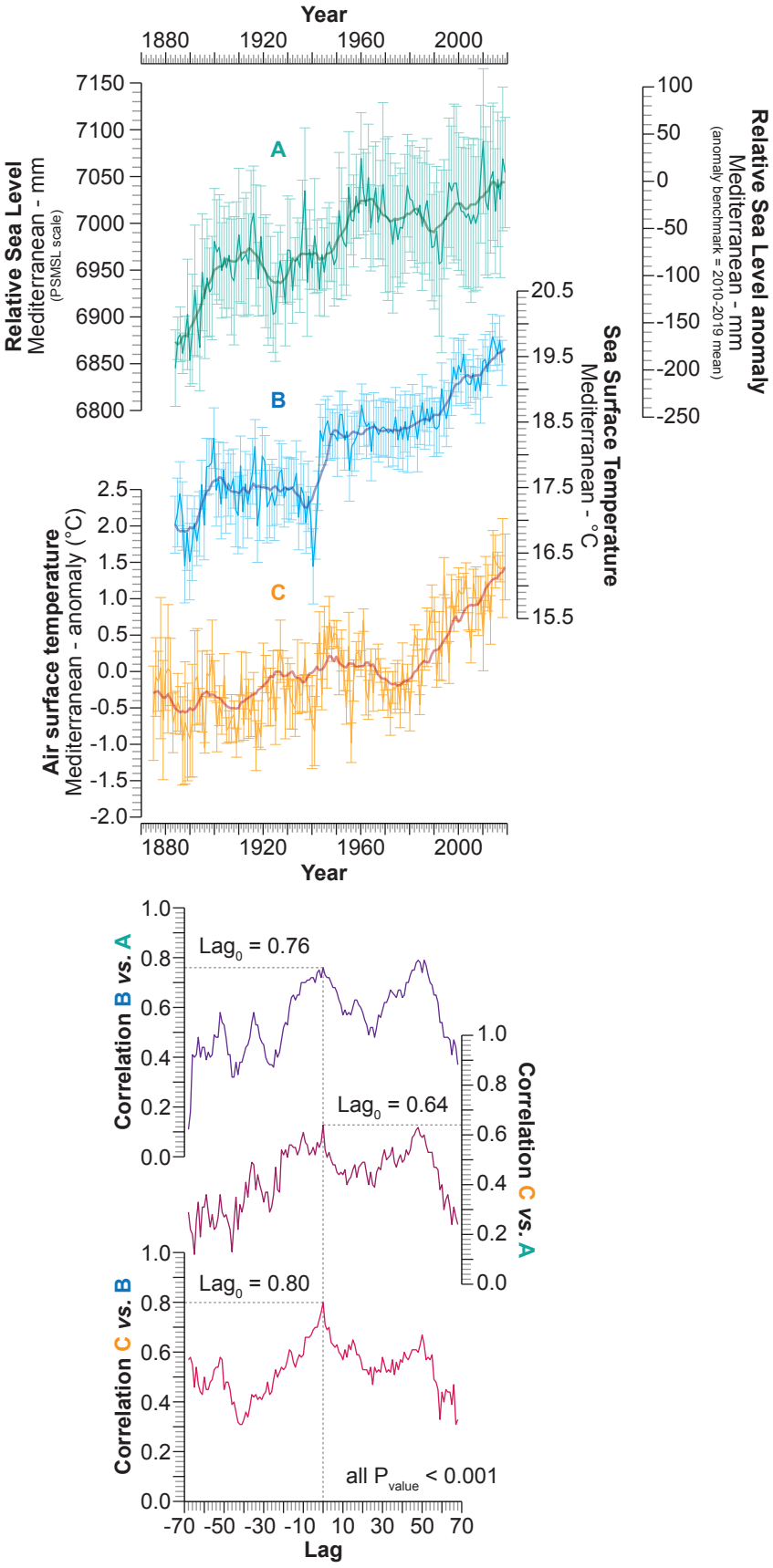

Figure 2: (A) Composite Mediterranean RSL stack for the period 1880-2020, produced using the 138 tide-gauge stations used in this study. **(B)** Composite stack of SSTs at the studied tide-gauge stations. **(C)** Mediterranean air surface temperatures (Osborn and Jones, 2014). The three bottom insets show the cross-correlations between the three considered variables.

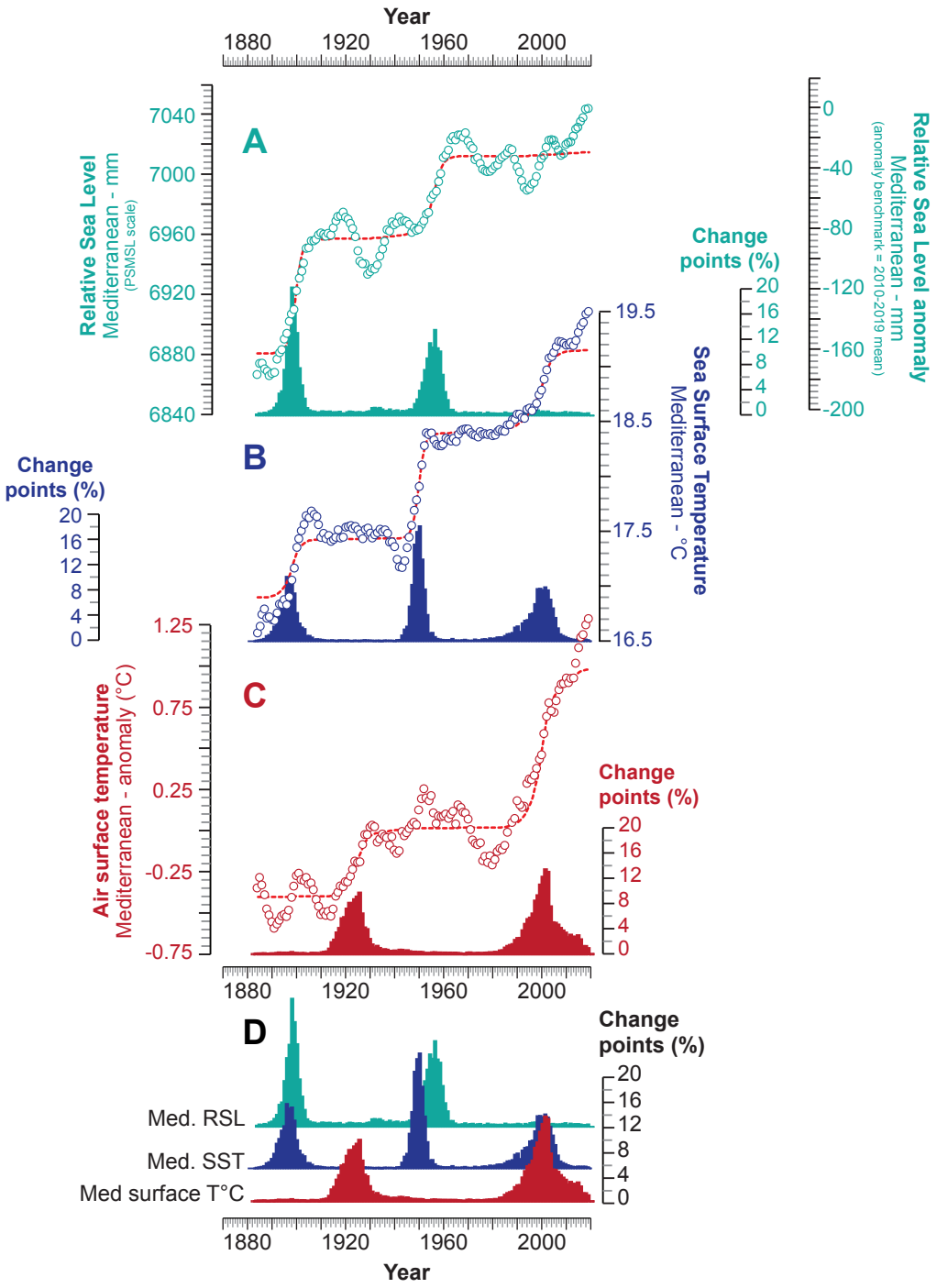

Figure 3: Change-point analysis of the Mediterranean RSL stack **(A)**, Mediterranean SSTs **(B)** and Mediterranean air surface temperatures **(C)**. **(D)** Juxtaposition of the different change points for the three time series.

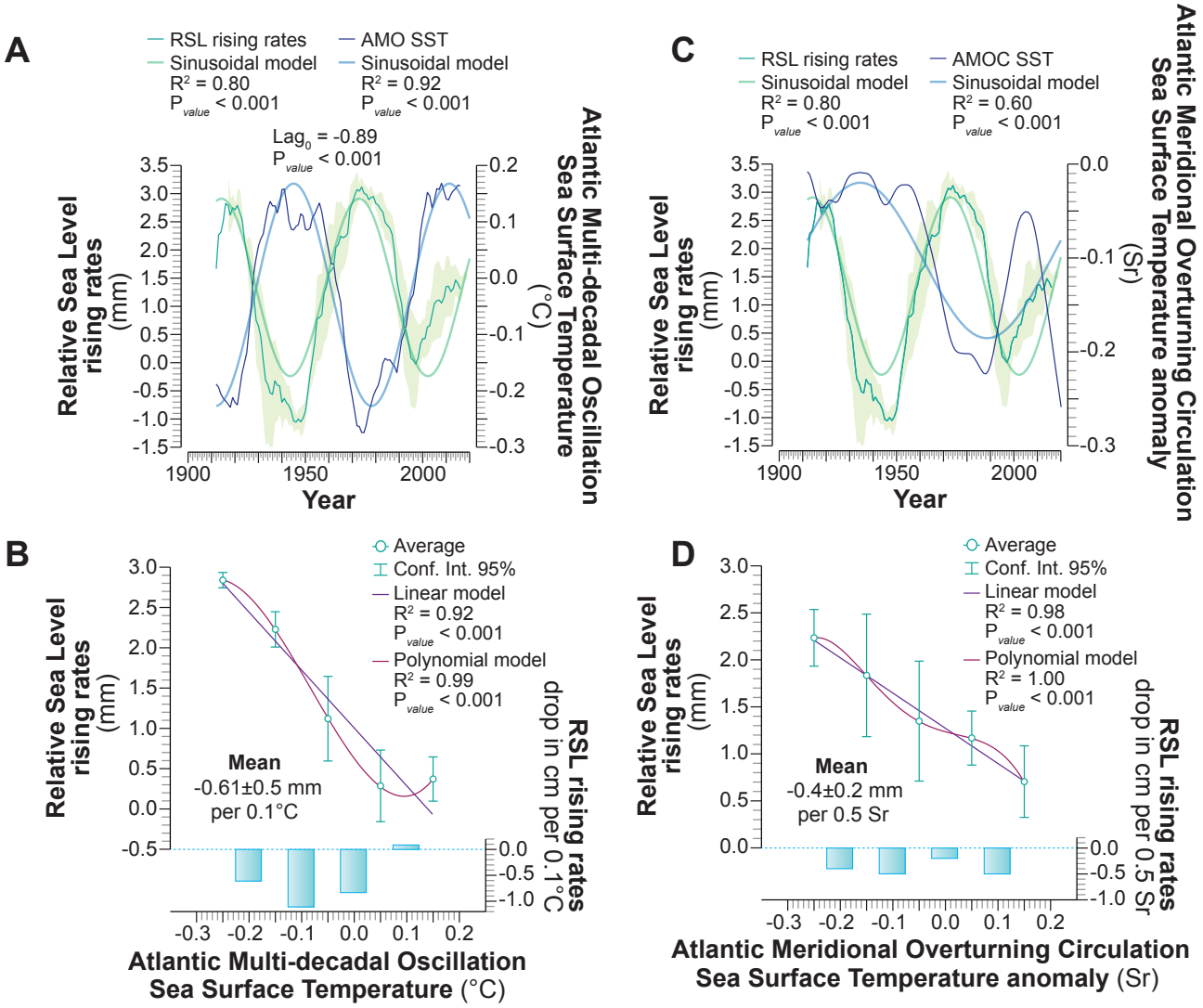

Figure 4: (A & B) Mediterranean relative sea-level rising rates (RSLRR) compared with Atlantic Multi-decadal Oscillation Sea Surface Temperature (°C; data from Enfield et al., 2001). **(C & D)** Mediterranean RSLRR versus Atlantic meridional overturning circulation Sea Surface Temperature anomaly (Sr; data from Caesar et al., 2018).

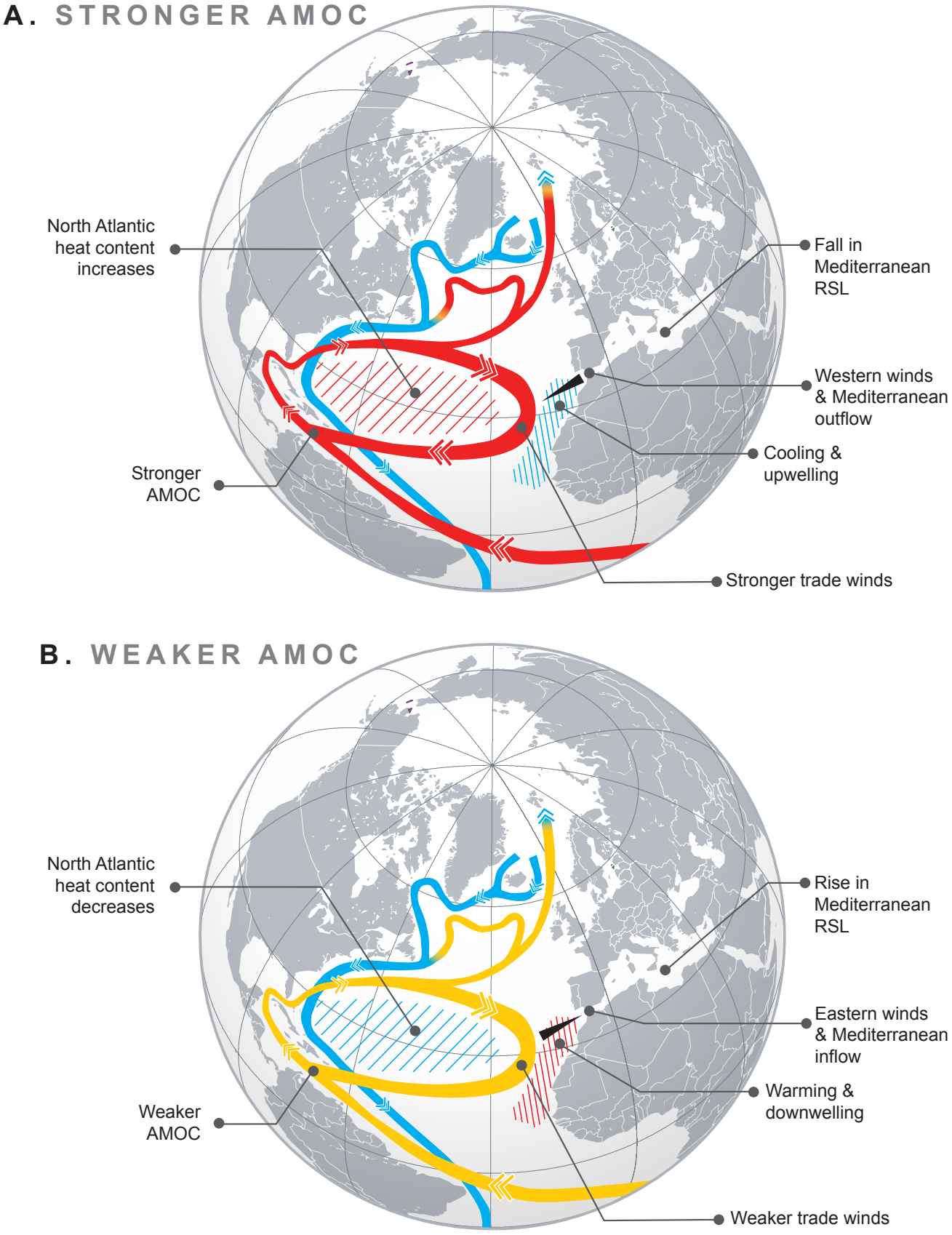

Figure 5: Schematic explanation of the climate/thermocline mechanisms leading to RSL changes in the Mediterranean during phases of stronger **(A)** and weaker **(B)** AMOC.

Supplementary Materials for

Forecasted weakening of Atlantic Overturning Circulation could amplify future relative sea-level rise in the Mediterranean: a review of climate and tide-gauge data links

Nick Marriner, David Kaniewski, Majid Pourkerman, Matteo Vacchi, Daniele Melini, Martin Seeliger, Christophe Morhange & Giorgio Spada

Correspondence to: nick.marriner@univ-fcomte.fr

This PDF file includes:

Figures S1 to S7

Other Supplementary Materials for this manuscript include the following:

Data S1

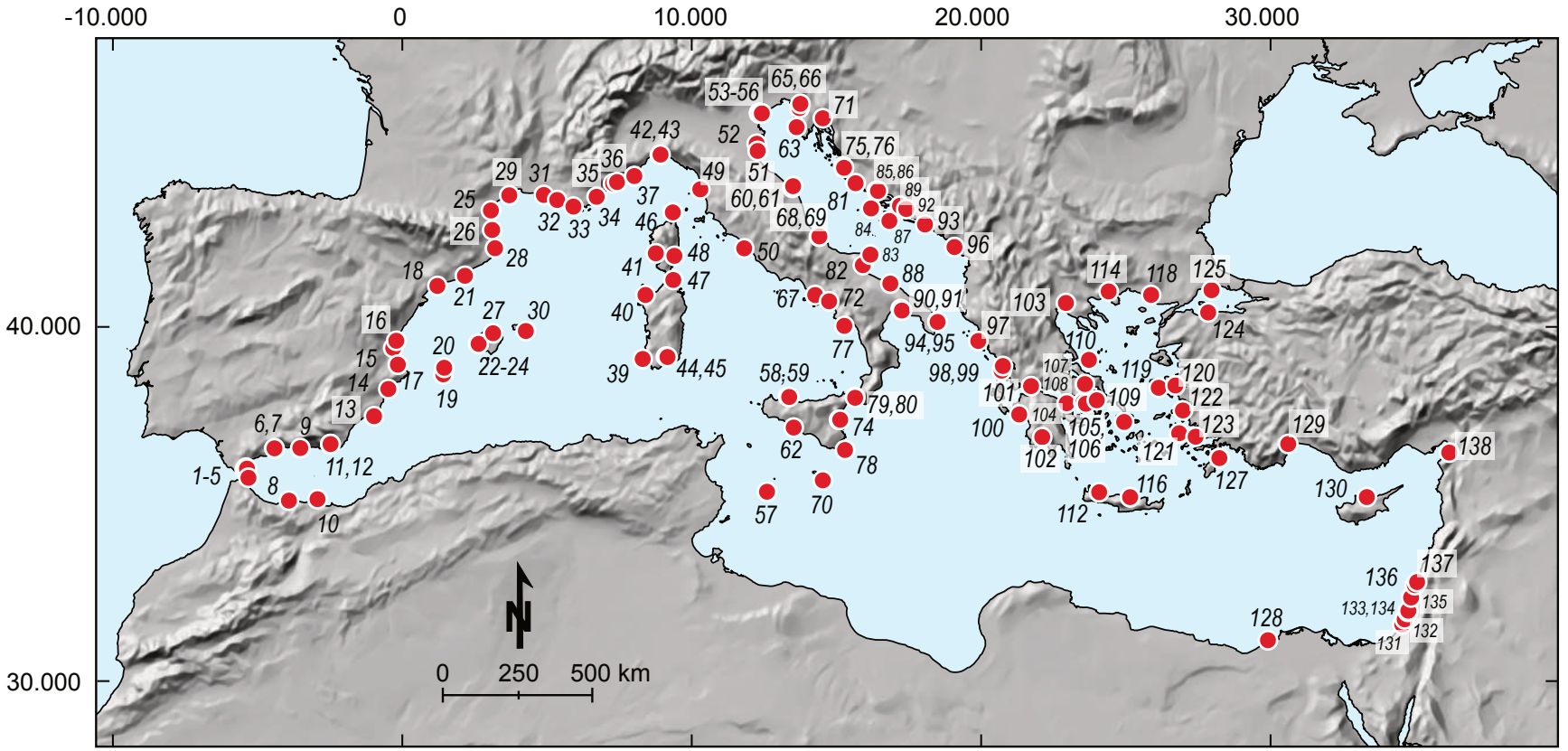

1. Algeciras B
2. Algeciras
3. Algeciras 2
4. Gibraltar
5. Ceuta
6. Malaga II
7. Malaga
8. Villa Sanjurjo
9. Motril
10. Melilla
11. Almeria
12. Almeria 2
13. Cartagena
14. Alicante
15. Valencia
16. Sagunto
17. Gandia
18. Tarragona
19. Formentera
20. Ibiza
21. Barcelona
22. Palma
23. Palma de Mallorca 2
24. Palma de Mallorca
25. Port la Nouvelle
26. Port Vendres
27. Alcudia
28. L'Estartit
29. Sete
30. Mahon
31. Fos sur Mer
32. Marseille
33. Toulon
34. Port Ferreol
35. Nice
36. Monaco Fontvieille
37. Porto Maurizio
38. Imperia
39. Carloforte
40. Porto Torres
41. Ajaccio
42. Genova
43. Genova II
44. Cagliari II
45. Cagliari
46. Centuri
47. La Maddalena
48. Solenzara
49. Livorno II
50. Civitavecchia
51. Porto Garibaldi
52. Porto Corsini
53. Venezia (S. Stefano)
54. Venezia (Punta Della Salute)
55. Venezia (Arsenale)
56. Venezia II
57. Lampedusa
58. Palermo
59. Palermo II
60. Ancona
61. Ancona II
62. Porto Empedocle
63. Rovinj
64. Koper
65. Luka Koper
66. Trieste
67. Napoli II
68. Ortona
69. Ortona II
70. Marsaxlokk
71. Bakar
72. Salerno
73. Catania II
74. Catania
75. Zadar
76. Gazenica
77. Palinuro
78. Capo Passero
79. Reggio Calabria II
80. Reggio Calabria
81. Zlarin
82. Manfredonia
83. Vieste
84. Vis-Ceska Vila
85. Split Rt Marjana
86. Split Gradska Luka
87. Ubli
88. Bari
89. Sucuraj
90. Taranto II
91. Taranto
92. Ploce
93. Dubrovnik
94. Otranto II
95. Otranto
96. Bar
97. Corfu
98. Levkas
99. Preveza
100. Katakolon
101. Patrai
102. Kalamai
103. Thessaloniki
104. Posidhonia
105. North Salaminos II
106. North Salaminos
107. Khalkis South
108. Khalkis North
109. Piraieus
110. Skopelos
111. Rafina
112. Soudhas
113. Soudhas II
114. Kavalla
115. Siros
116. Iraklion
117. Iraklion II
118. Alexandroupolis
119. Khios
120. Mentes_Izmir
121. Leros
122. Samos
123. Bodrum II
124. Erdek
125. Marmara
126. Rhodos
127. Rhodos II
128. Alexandria
129. Antalya II
130. Girne
131. Ashklon
132. Ashdod II
133. Tel Aviv - Yafo
134. Tel Aviv
135. Hadera
136. Haifa II
137. Akko
138. Iskenderun II

Fig. S1: Location of tide gauge stations used in the present study. The stations have been numbered 1 to 138 and sorted by longitude, with 1 being furthest west and 138 the station furthest east.

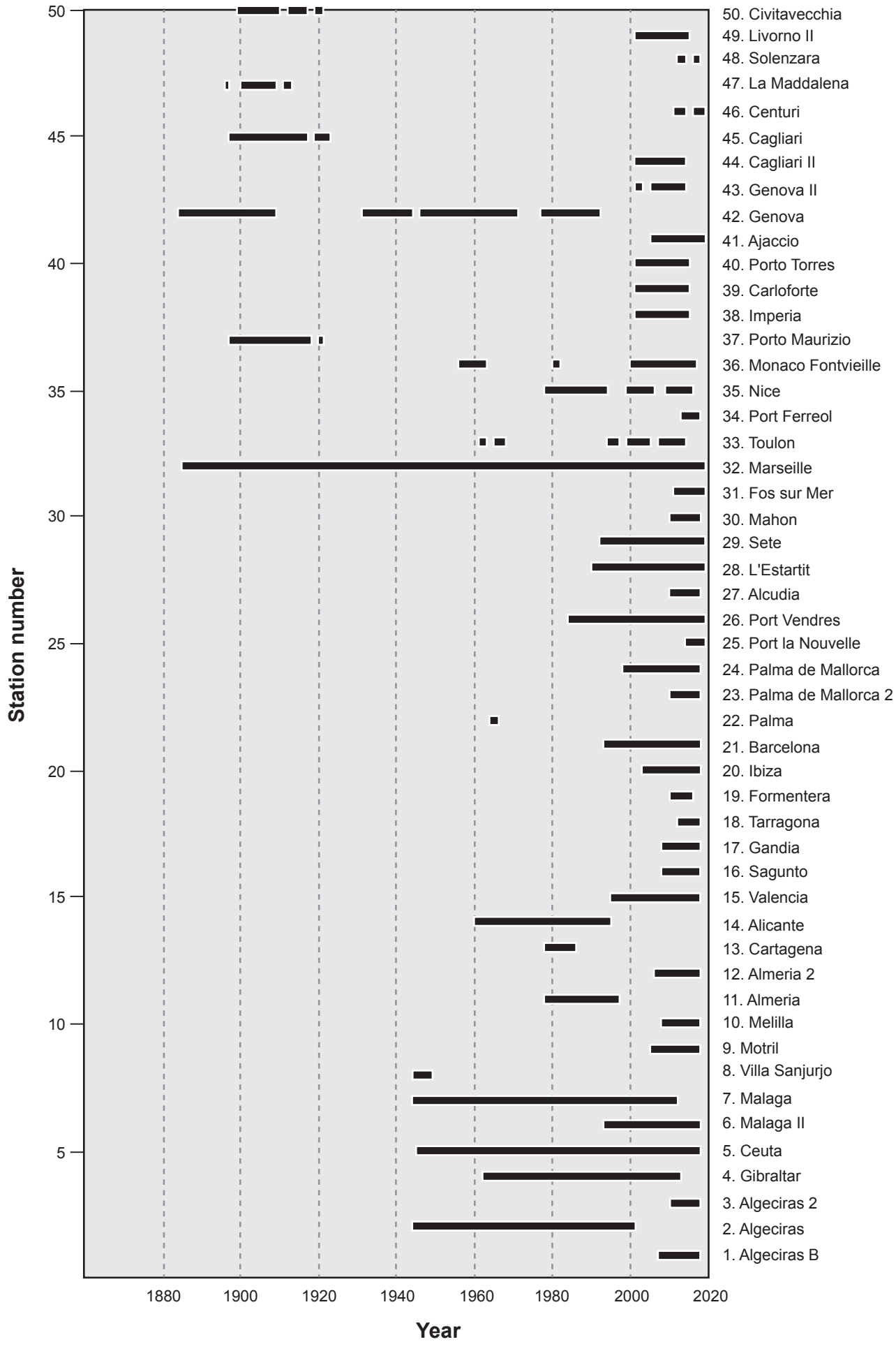

Fig. S2: Temporal coverage of tide gauge records for stations 1 to 50.

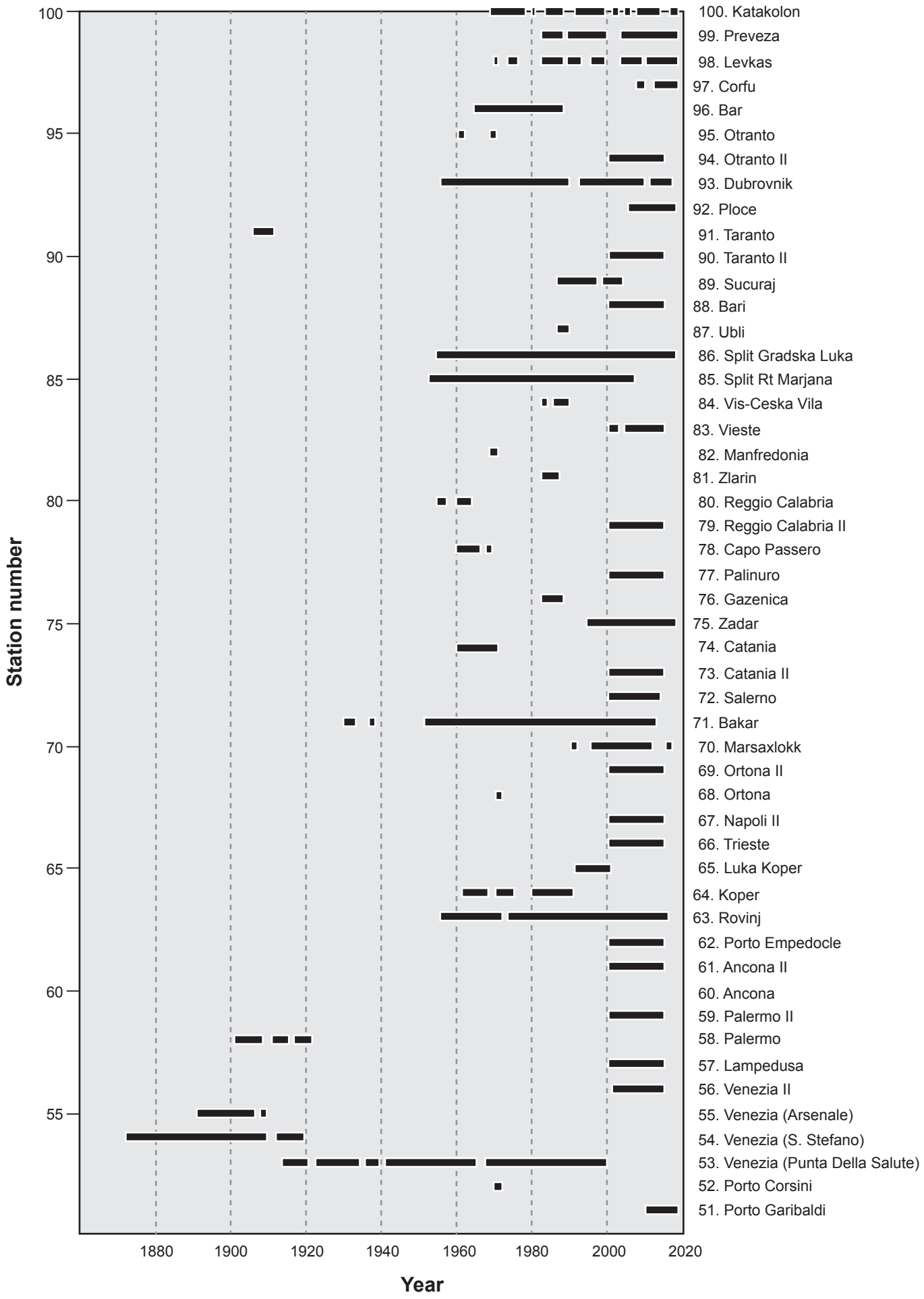

Fig. S3: Temporal coverage of tide gauge records for stations 51 to 100.

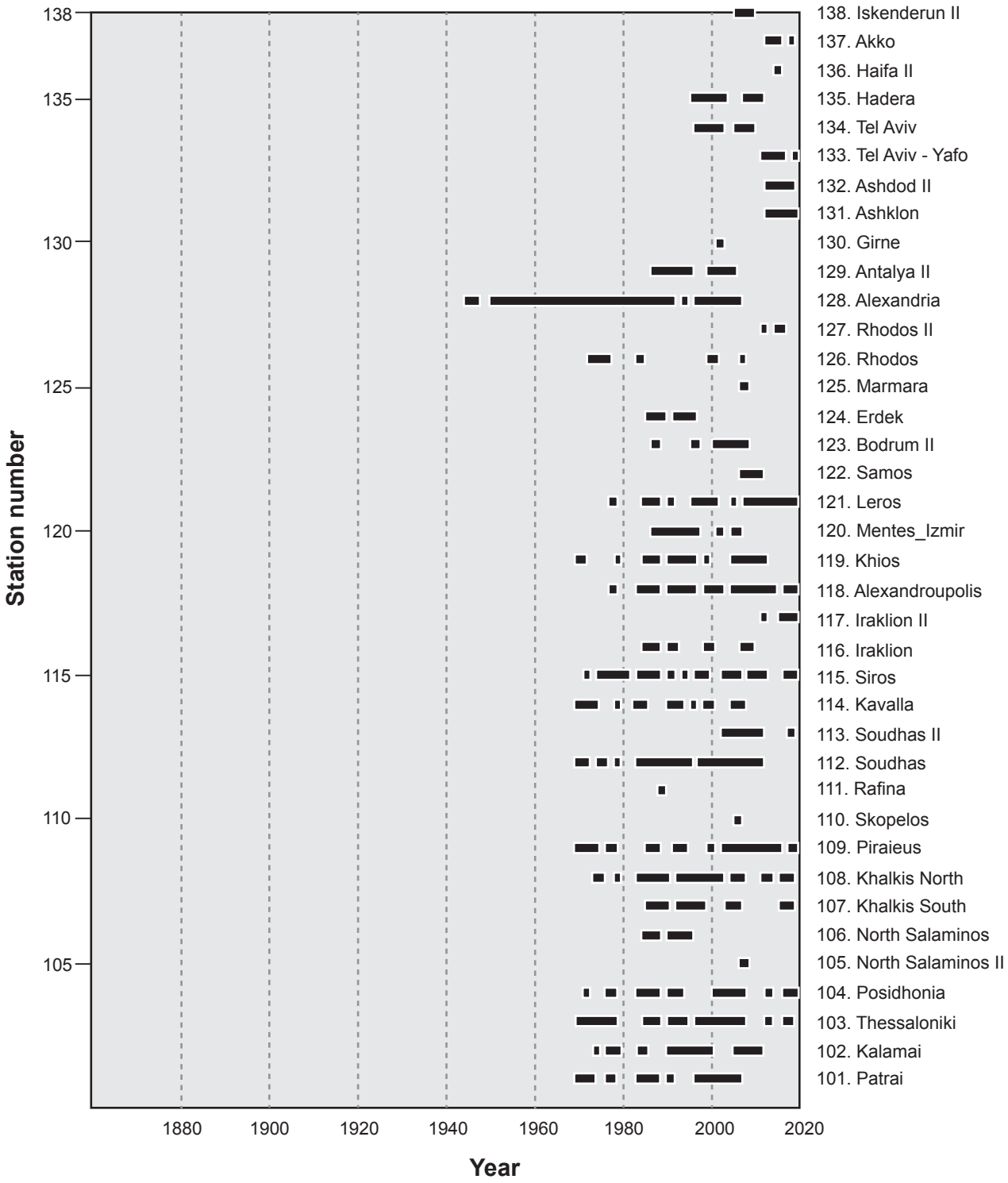

Fig. S4: Temporal coverage of tide gauge records for stations 101 to 138.

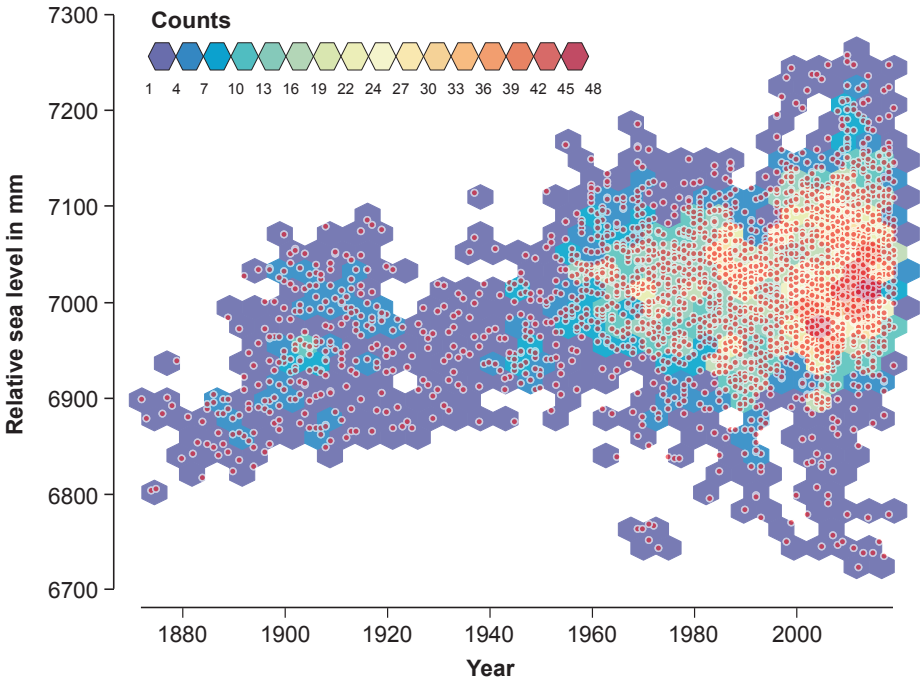

Fig. S5: Plot of Mediterranean RSL data from the 138 Mediterranean tide-gauge stations used in this study.

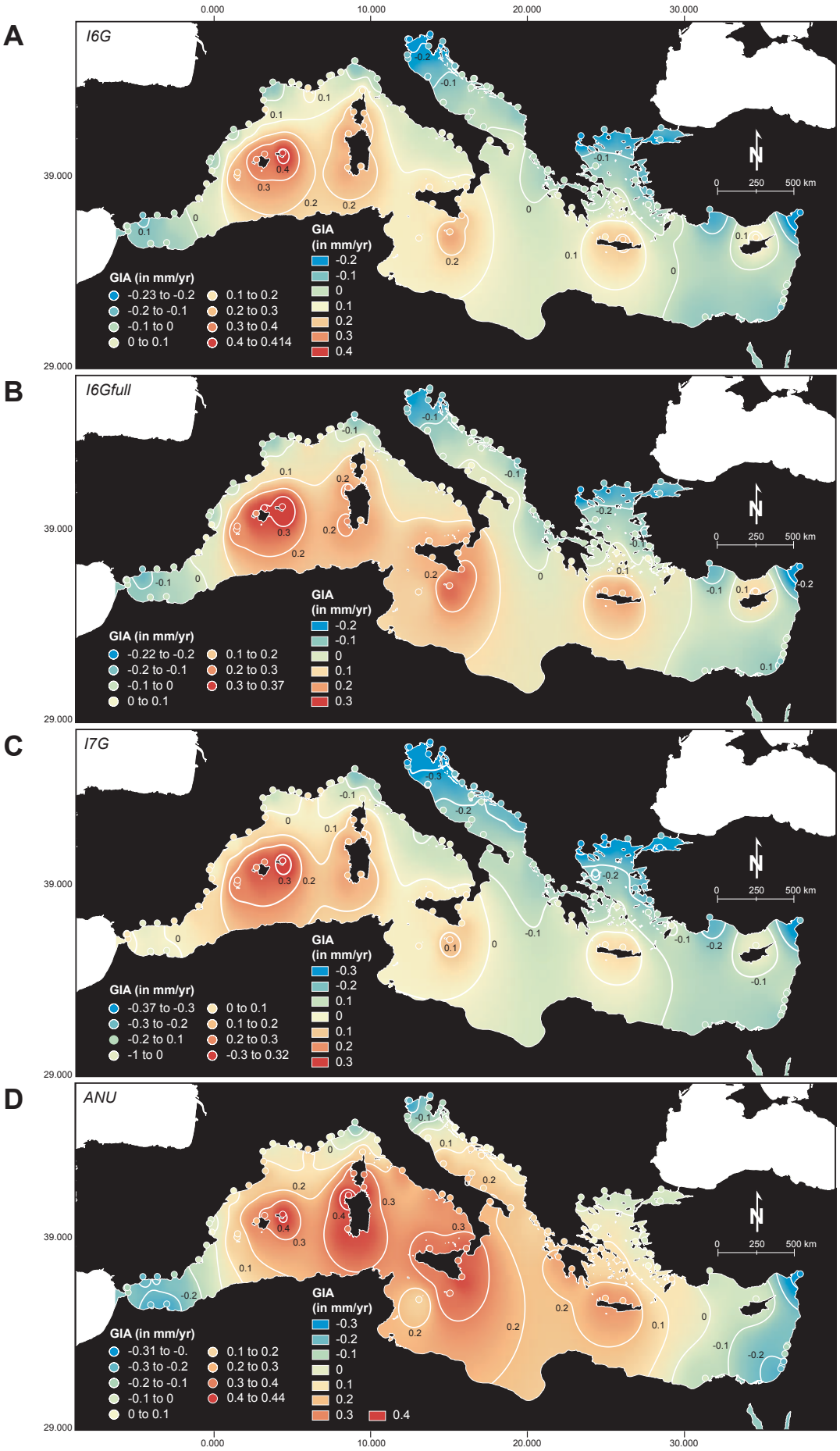

Fig. S6: Present-day rates of sea level change in the Mediterranean area according to a set of Glacial Isostatic Adjustment models: **(A)** the ICE-6G model since the last glacial maximum (Peltier et al., 2015), **(B)** the ICE-6G model over the full last glacial cycle, **(C)** the ICE-7G model (Roy and Peltier, 2018) and **(D)** one of the models progressivley developed by the Australian National University (ANU) research group (Lambeck et al., 2003; Nakada and Lambeck, 1987). The white dots denote the location of tide gauges used in the study.

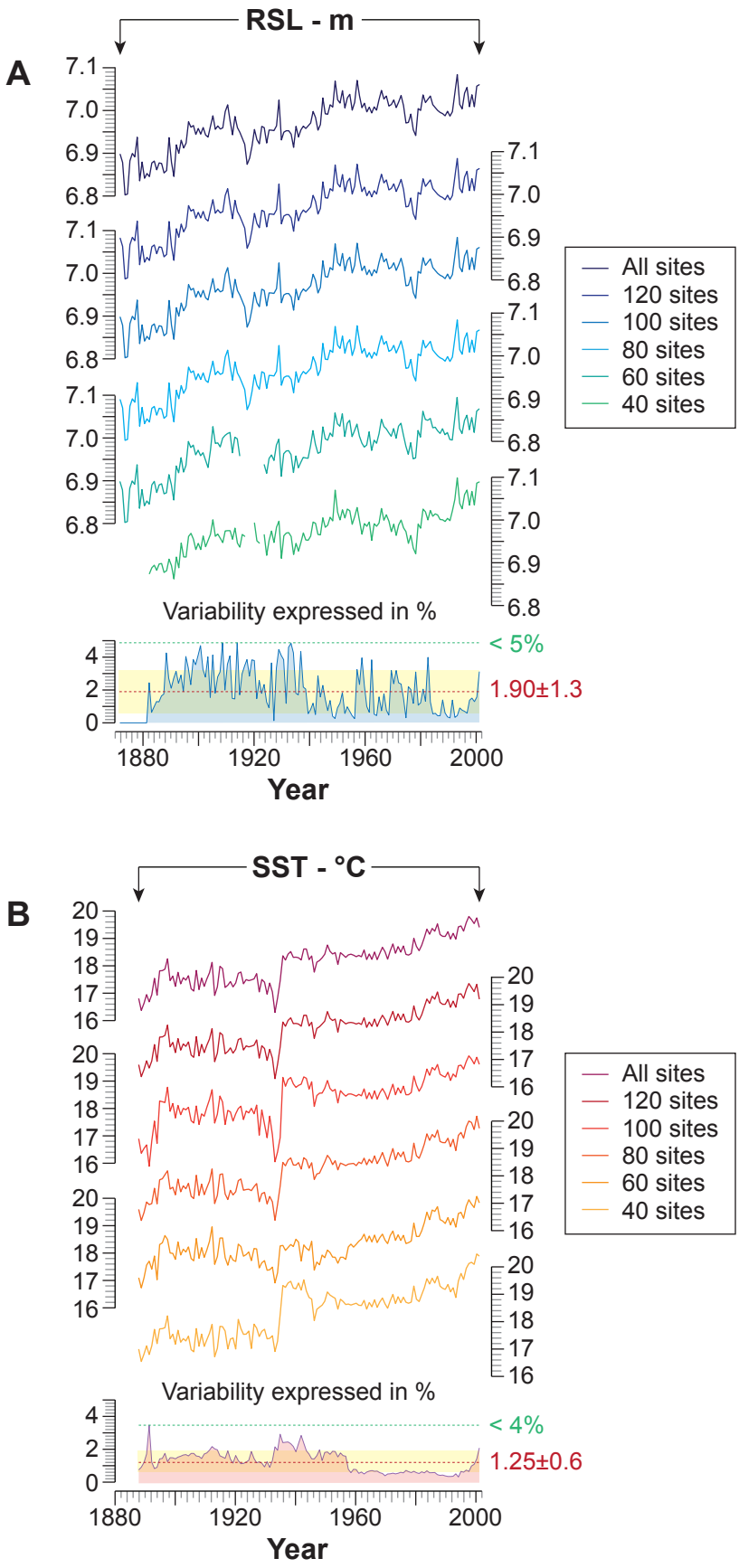

Fig. S7: Effects of random sampling on the reconstructed Relative Sea Level (RSL) **(A)** and Sea Surface Temperature (SST) **(B)** time series. The figure shows five sub-sampled time series of 40, 60, 80, 100, and 120 records, out of a total of 138 records. Our analysis indicates that the overall variability between the sub-sampled time series and the "all sites" series was minimal. Specifically, for the RSL record, the overall variability was less than 5% (mean = 1.57 ± 1.1%), while for the SST record, the overall variability was less than 4% (mean = 1.25 ± 0.6%).